A Portable Anaerobic Microbioreactor Reveals Optimum Growth Conditions for the Methanogen *Methanosaeta concilii*[∇]

Benjamin Steinhaus,[1] Marcelo L. Garcia,[2] Amy Q. Shen,[1] and Largus T. Angenent[2]*

Department of Mechanical and Aerospace Engineering, Washington University in St. Louis, St. Louis, Missouri 63130,[1] and Department of Energy, Environmental and Chemical Engineering, Washington University in St. Louis, St. Louis, Missouri 63130[2]

Conventional studies of the optimum growth conditions for methanogens (methane-producing, obligate anaerobic archaea) are typically conducted with serum bottles or bioreactors. The use of microfluidics to culture methanogens allows direct microscopic observations of the time-integrated response of growth. Here, we developed a microbioreactor (μBR) with ~1-μl microchannels to study some optimum growth conditions for the methanogen *Methanosaeta concilii*. The μBR is contained in an anaerobic chamber specifically designed to place it directly onto an inverted light microscope stage while maintaining a N_2-CO_2 environment. The methanogen was cultured for months inside microchannels of different widths. Channel width was manipulated to create various fluid velocities, allowing the direct study of the behavior and responses of *M. concilii* to various shear stresses and revealing an optimum shear level of ~20 to 35 μPa. Gradients in a single microchannel were then used to find an optimum pH level of 7.6 and an optimum total NH_4-N concentration of less than 1,100 mg/liter (<47 mg/liter as free NH_3-N) for *M. concilii* under conditions of the previously determined ideal shear stress and pH and at a temperature of 35°C.

Microfluidic networks have recently gained importance for their wide variety of microbial applications. For example, microchannels were used by DiLuzio et al. (11) to examine the swimming behavior of *Escherichia coli*. DiLuzio et al. showed that *E. coli* sensed the presence of channel walls at distances of up to 10 μm. Balagaddé et al. (5) built a microfluidic bioreactor containing a feedback control loop, which was able to correlate sustained oscillation in the cellular density of planktonic *E. coli* with morphological changes. The microfluidic networks used in these studies allowed researchers to directly observe the responses of microbial cells to various stimuli and provided new and unique insights into the growth and behavior of these cells. The use of microfluidics has become practicable because of the development of an inexpensive, biocompatible, and transparent but readily diffusive polymeric material (i.e., polydimethylsiloxane [PDMS]), which is used to construct micron-scale fluid networks in virtually any two-dimensional configuration (12, 23). Due to the extensive gas permeability of PDMS and the elevated cost of nondiffusive materials to construct microchannels, the application of microfluidics to the study of the growth and behavior of anaerobic microorganisms has been hindered.

Conventional studies of the behavior of anaerobes, their responses to various stimuli, and their attachment have been performed with medium bottles or bioreactors ranging anywhere from several milliliters to several liters in size (2, 3, 6, 24). These systems serve to provide the anaerobic conditions necessary for growth. They do not, however, allow for any type of direct observation (without sampling disturbance) of mi-crobe behavior, morphology, or the ability to attach to a matrix during growth. By utilizing microfluidics, real-time observations, impossible with current culture techniques, may be made of an anaerobe's response to various growth stimuli.

We have developed an anaerobic microbioreactor (μBR), utilizing conventional microfluidics in combination with a transparent anaerobic chamber, which can be placed on an inverted light microscope stage. To test this μBR, we used the methanogen *Methanosaeta concilii*, which is particularly well suited for testing our anaerobic system because it is one of the strictest anaerobes (13), able to survive only at extremely low O_2 concentrations (15). *M. concilii* has single cellular dimensions of 0.8 by 2.5 μm. These cells grow end-to-end into long filaments of 100 μm or more in length, with a doubling time of ~1 day under optimal conditions (22). *M. concilii* filaments may in turn organize into large bundles or clumps (3, 16); however, this did not occur in our study. In total, six runs were performed with *M. concilii*, two to determine ideal flow conditions (S1 and S2), two to determine the optimal pH (PH1 and PH2), and two to determine the inhibiting ammonia conditions (A1 and A2).

Two different microfluidic geometries were employed (Fig. 1): a shear geometry for S1 and S2 with various channel widths, generating fluid velocities that varied over 2 orders of magnitude, and a gradient geometry for determining optimum medium properties (PH1, PH2, A1, and A2). The mixing regimen in this geometry creates nine clearly defined bands with different concentrations in a single microchannel. We investigated these bands with a green fluorescent dye and found no convective mixing of the dye between the bands due to a laminar flow in the microchannels. Based on the findings from runs S1 and S2, we utilized an ideal shear stress of ~31 μPa at a flow rate of 0.010 ml/h for runs PH1, PH2, A1, and A2. Similarly, the optimal pH level of 7.6, which was found in runs PH1 and PH2, was utilized for runs A1 and A2.

* Corresponding author. Mailing address: Washington University in St. Louis, One Brookings Drive, Campus Box 1180, St. Louis, MO 63130. Phone: (314) 935-5663. Fax: (314) 935-5464. E-mail: angenent @seas.wustl.edu.
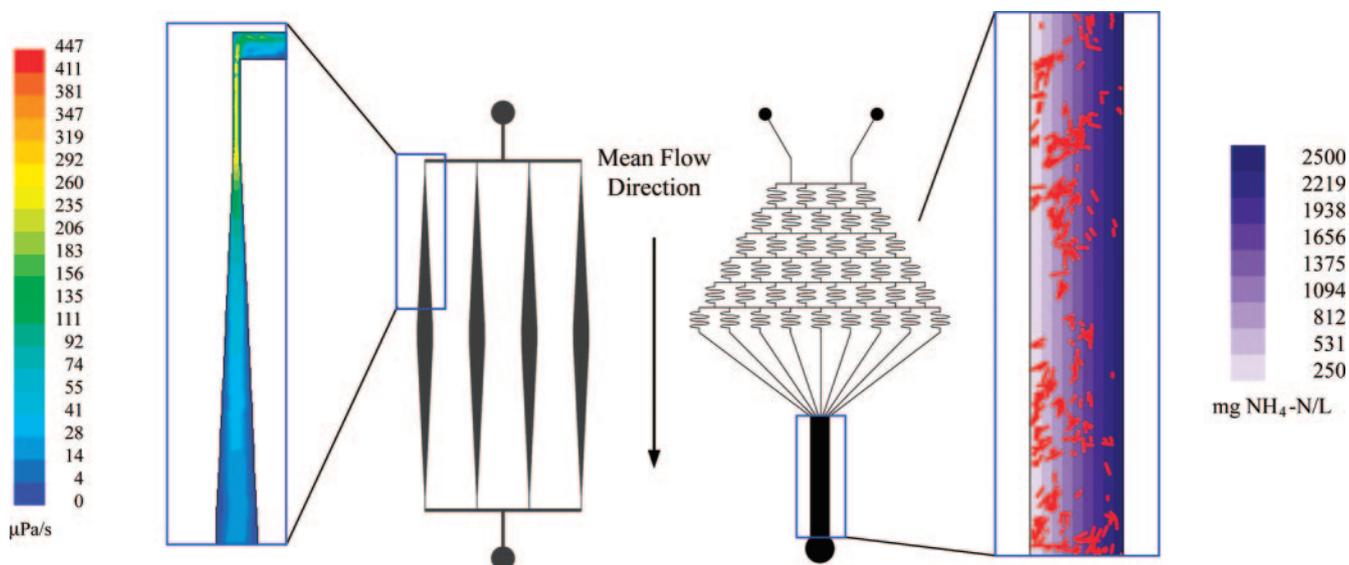
FIG. 1. Microfluidic geometries used for the shear stress (left) and gradient (right) studies. Insets show computational fluid dynamics modeling (FLUENT, Lebanon, NH) of the shear stress contours in the shear reactor (left) and a recreation of the microfluidic ammonia gradient contours with filaments (right) (filament width not to scale).

MATERIALS AND METHODS

Microbioreactor and anaerobic chamber. The microfluidic network used for the shear stress studies was comprised of four channels with widths varying from 0.050 to 1 mm, a depth of 0.1 mm, a length of 20 mm, and a volume of 1 μl. The second geometry (for optimum pH and ammonia level studies) utilized small-scale fluid gradients created by a fluid network with two inlet channels followed by a complex mixing region. In this mixing region, the two inlet fluids were split, combined, mixed, and split again six times, creating nine fluid streams leaving the mixing region. This mixing region fed into an outlet channel with a width of 1.5 mm, a depth of 0.1 mm, a length of 9 mm, and a volume of 1.4 μl (Fig. 1). The microchannels used in the μBR were produced using standard soft-lithography techniques (12, 23). PDMS was poured over a patterned substrate, cured for 1 h at 60°C to form a negative imprint of the pattern, and then removed and permanently bound to a glass slide, forming a closed fluid network. An anaerobic chamber with inside dimensions of 13.3 by 13.3 by 1.6 cm was constructed from

acrylic (Fig. 2) to maintain the microchannels under anaerobic conditions. The lid of the chamber was held in place by thumbscrews and placed on an O-ring covered in silicone grease to ensure a positive pressure inside the chamber.

A syringe pump (PHD 2000; Harvard Apparatus, Boston, MA) supplied substrate medium through polyethylene oxide (PEO) tubing (PE 20; Becton Dickenson, Sparks, MD) to the microchannels via a side port in the anaerobic chamber. To prevent oxygen from diffusing from the atmosphere through the PEO into the growth medium, the PEO tubing was placed in 1.3-cm-diameter Norprene tubing (Cole-Parmer, Chicago, IL) (Fig. 2). The ends of the Norprene tubing were pulled over the barrels of gas-tight 5-ml gas chromatographic syringes (Fisher Scientific, Houston, TX) and the inlet hose barbs. A T-junction was connected to the Norprene hose barb, the anaerobic chamber, and the regulator of an 80%:20% N_2-CO_2 tank. The gas line purged the tubing and anaerobic chamber for 3 s every 30 min via a solenoid valve attached to a timer (Chrontrol, San Diego, CA). A bubbler was connected to a second side port in
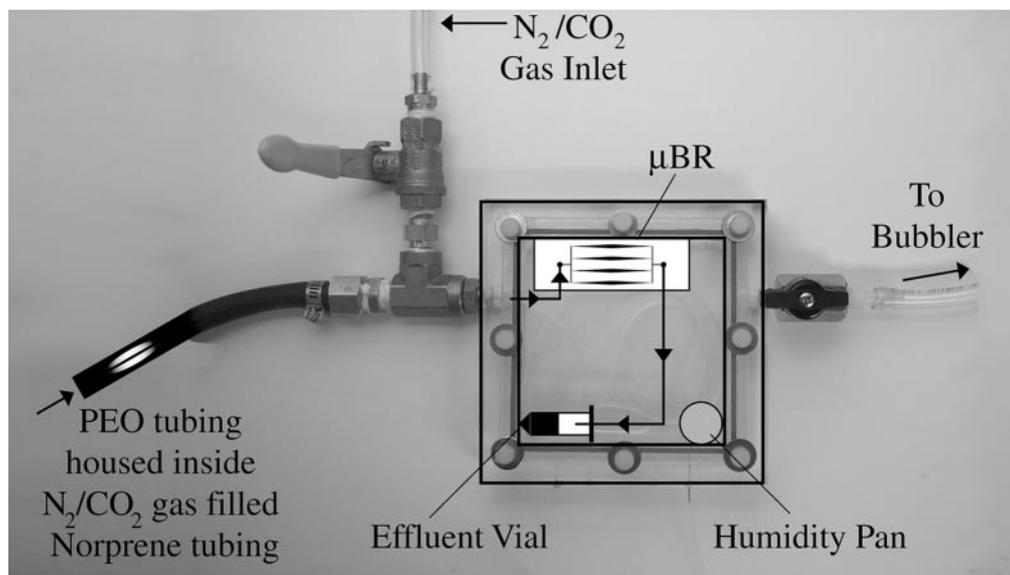

FIG. 2. Anaerobic chamber setup housing the μBR.

TABLE 1. Parameters for each of the six experiments conducted using μBR

Run name	Microfluidic geometry	Flow rate (ml/h)	pH	Ammonia level (mg N/liter)	Duration (wk)
S1	Shear	0.005	7.0	250	12
S2	Shear	0.010	7.0	250	8
PH1	Gradient	0.010	5.5–8.0	250	5
PH2	Gradient	0.010	6.5–8.5	250	3
A1	Gradient	0.010	7.5	250–2,500	1
A2	Gradient	0.010	7.5	250–2,500	4

the anaerobic chamber to maintain a positive pressure. A 2-ml centrifuge vial and a 15-ml test tube cap were then placed in the chamber to serve as a waste receptacle and humidity pan, respectively. The 15-ml test tube cap was filled with ~1.5 ml of a sodium sulfide (0.05%, wt/vol) and cysteine-HCl (0.05%, wt/vol) solution to prevent the microchannels from drying out and to help scavenge any residual oxygen.

Methanosaeta concilii. *M. concilii* strain GP6 was obtained from the Portland State University collection (Beaverton, OR). A growth medium was made from the procedure posted by the DSMZ (Braunschweig, Germany) for *Methanothrix* (medium 334) and was prepared both aseptically and anaerobically. The medium consisted of (per liter of deionized water) sodium acetate, 6.800 g; KH_2PO_4, 0.300 g; NaCl, 0.600 g; $MgCl_2 \cdot 6H_2O$, 0.100 g; $CaCl_2 \cdot 2H_2O$, 0.080 g; NH_4Cl, 1.000 g; and $KHCO_3$, 4.000 g; as well as trace metal (1 ml) and vitamin (1 ml) solutions. The trace metal solution contained (per liter of deionized water) nitrilotriacetic acid, 12.800 g; $FeCl_3 \cdot 6H_2O$, 1.350 g; $MnCl_2 \cdot 4H_2O$, 0.100 g; $CoCl_2 \cdot 6H_2O$, 0.024 g; $CaCl_2 \cdot 2H_2O$, 0.100 g; $ZnCl_2$, 0.100 g; $CuCl_2 \cdot 2H_2O$, 0.025 g; H_3BO_3, 0.010 g; $Na_2MoO_4 \cdot 2H_2O$, 0.024 g; NaCl, 1.000 g; $NiCl_2 \cdot 6H_2O$, 0.120 g; and $Na_2SeO_3 \cdot 5H_2O$, 0.026 g. The vitamin solution was comprised of (per liter of deionized water) biotin, 2.000 mg; folic acid, 2.000 mg; pyridoxine-HCl, 10.000 mg; thiamine-HCl $\cdot$ $2H_2O$, 5.000 mg; riboflavin, 5.000 mg; nicotinic acid, 5.000 mg; D-Ca-pantothenate, 5.000 mg; vitamin B_{12}, 0.100 mg; *p*-aminobenzoic acid, 5.000 mg; and lipoic acid, 5.000 mg. Resazurin (1 mg per liter) was added into the medium as an O_2 indicator. The antibiotics streptomycin (0.005%, wt/vol) and chloramphenicol (0.02%, wt/vol) as well as the antifungal agent cycloheximide (0.004%, wt/vol) were also added to the medium.

Start-up and operating conditions. Start-up procedures were identical for both microfluidic geometries. The channels were retreated with plasma gas, rendering them hydrophilic, and immediately filled with sterile deionized water. They were then placed inside the anaerobic chamber and connected to the PEO tubing, after which the anaerobic chamber was sealed. The chamber, including the μBR, was subsequently exposed to UV light in a microbial hood for ~15 min to sterilize the channels and placed in an anaerobic hood. The microchannels were flushed with ~0.1 ml of a sodium sulfide (0.05%, wt/vol) and cysteine-HCl (0.05%, wt/vol) solution followed by 0.1 ml of medium. Next, the channels were flushed with 0.25 ml of inoculum directly from the Portland State University culture. Finally, glass gas chromatographic syringes were filled with medium, attached to the needle tips and Norprene tubing, and placed in the syringe pump. After the system was sealed and placed in the 35°C incubator, the reactor was left without flow for 24 h before being perfused with medium. The operating conditions were amended according to the type of experiment (Table 1).

Data analysis. Observations were made when the anaerobic chamber with the μBR was removed from the incubator and examined with a Leica inverted light microscope (model DMIRB; Wetzlar, Germany) once every 7 days. Pictures were taken at a magnification of ×100 using a QICam and the OpenLab imaging system (QImaging, Burnaby, British Columbia, Canada). Each individual image file was then compiled into a single video file (with an .avi extension) using MGI VideWave4 (Sonic Solutions, Santa Clara, CA). Dimensions were extracted from the video files and analyzed using Photron data analysis software (Photron USA, Inc., San Diego, CA).

Filament lengths for the shear study were determined by marking the endpoints of each individual filament. Channel widths at which filaments were growing were then determined by bisecting each filament using a line with endpoints on the channel wall. Each individual point was converted into a set of *x*, *y* coordinates with pixels as the positional units, and distances were converted from pixels to microns with a calibration slide. This analysis yielded a measure of filamentous density (number of filaments/mm²) as a function of channel width. Shear stresses were calculated using a standard correlation for wall shear stress,

$τ_w$, which assumes that the fluid flow is viscous, laminar, and incompressible, by using the following equation (21):

$$\tau_w = 0.332 u^{\frac{3}{2}} \sqrt{\frac{\rho\mu}{y}} \qquad (1)$$

where *u* is the fluid velocity, ρ is the fluid density, μ is the fluid viscosity, and *y* is the distance from the wall, which was estimated as the average cellular height (normal to the channel wall).

For the gradient studies, *M. concilii* filament lengths were often longer than the widths of the individual gradients (Fig. 1, right channel). We therefore obtained an overall cellular density (number of cells/mm²) instead of filamentous density. First, filament length was determined similarly to the way it was determined in the shear study. Second, to find the position of the filament in the channel, the tip of each filament was marked and connected to the channel wall to determine *x*, *y* coordinates. Third, the *x*, *y* coordinates were run through a Matlab code (The Mathworks, Inc., Natick, MA), which broke each filament apart into individual cells based on the average size of a single cell. This gave each cell its own position and yielded cellular density as a function of position with respect to the channel wall.

To determine the optimal pH level, Igor Pro (Portland, OR) was used to fit the data to a Gaussian curve, as follows:

$$y = y_0 + Ae\left[-\left(\frac{x - x_0}{w}\right)^2 \right] \qquad (2)$$

where *x* is the pH, *y* is the cellular density, x_0 corresponds to the *x* position of the curve's peak (in this case the maximum pH), *A* is the maximum change in the curve's height, y_0 is the minimum curve height (or minimum cellular density), and *w* is the curve width.

RESULTS AND DISCUSSION

Effects of microchannel surface properties on the attachment of *M. concilii*. By using a microfluidic system to culture anaerobes, we monitored *M. concilii* filament densities on an inverted light microscope stage without sampling disturbance. For example, we tested the effect of microchannel surface properties on *M. concilii* adherence. The hydrophobic character of *M. concilii* has a considerable effect on its behavior. Previous studies have shown that in polar liquids, such as our media, cellular adhesion of *M. concilii* is ideal on hydrophilic surfaces (1, 28, 29). To verify this and to optimize the adherence of *M. concilii* in our microchannels, we operated μBR systems with both hydrophobic and hydrophilic (plasma-treated) surfaces. We found that channels with hydrophilic surfaces had a positive effect on the initial adherence of *M. concilii* inside the μBR channel (data not shown). Therefore, all of our microfluidic networks were plasma treated prior to use.

Despite the plasma treatment step, the overall filamentous density of the reactor was high immediately after inoculation with *M. concilii* and dropped to a low uniform level after medium flow was initiated. From this lower cellular density level, an enriched filament density began to appear based on the location of the ideal growth conditions for *M. concilii*. The duration of cellular washout depended on initial filamentous density levels after inoculation, governing the total length of the operating period (Table 1). For example, for run S2, large amounts of partially attached *M. concilii* cells were washed out of the system during the first 4 weeks of the operating period. The regions of optimal growth began to emerge after 5 weeks (Fig. 3), and the final data were reported after 8 weeks. In comparison, run A1 was completed in only 1 week (Table 1).

Effects of shear stress on *M. concilii* attachment. Runs S1 and S2 showed a clear effect of shear stress on filament density.
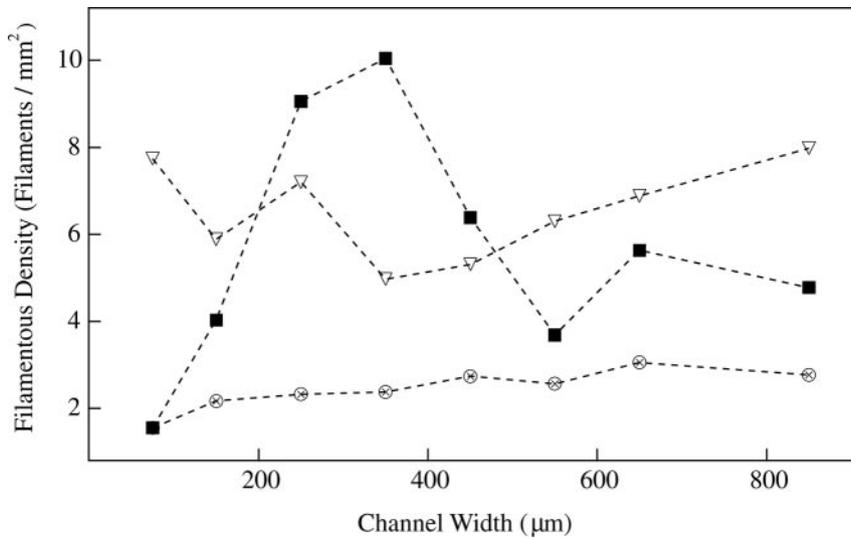
FIG. 3. Filamentous density as a function of channel width for run S2. Average data for weeks 1 and 2 ($\triangledown$), weeks 3 and 4 ($\otimes$), and weeks 5 and 6 ($\blacksquare$).

A maximum biomass density occurred at a shear level of ~20 to 35 μPa (Fig. 4), because *M. concilii* filaments were adhering more poorly to the microchannel surfaces under high shear stress in narrower channels, while they were growing more slowly at the low-medium turnover in the wider channels. Mixed-community biofilms can exist under shear stresses that are between ~2×10^3 and ~5×10^5 μPa (18, 25), indicating a much stronger attachment than that of the individual *M. concilii* filaments. The dynamics of cellular detachment under different conditions, such as shear stress, have been studied in microfluidic devices (19, 20, 26). Leclerc et al. (19), for example, found considerable cellular detachment with osteoblasts at a flow rate of 2.1 ml/h and adverse growth effects due to oxygen limitations at a lower flow rate of 0.3 ml/h.

Optimum pH levels for *M. concilii* growth. Chung et al. (9) created a microfluidic gradient of epidermal and fibroblast growth factor to search for the optimal levels required for neural stem cell growth. We utilized a similar gradient pattern to study some chemical optimum growth conditions for *M. concilii*. Our results from pH gradients between 5.5 and 8.5 were in excellent agreement with previously published data from Huser et al. (16), who obtained a pH optimum by measuring methane production rates in serum bottles with different pH values. This congruence is illustrated in Fig. 5, where our data from runs PH1 and PH2 are shown overlaid with the data of Huser et al. (16) along with the Gaussian curve fittings for all three data sets. We found agreement between all data sets, corresponding to an optimum pH level of 7.6 to 7.7 (the opti-
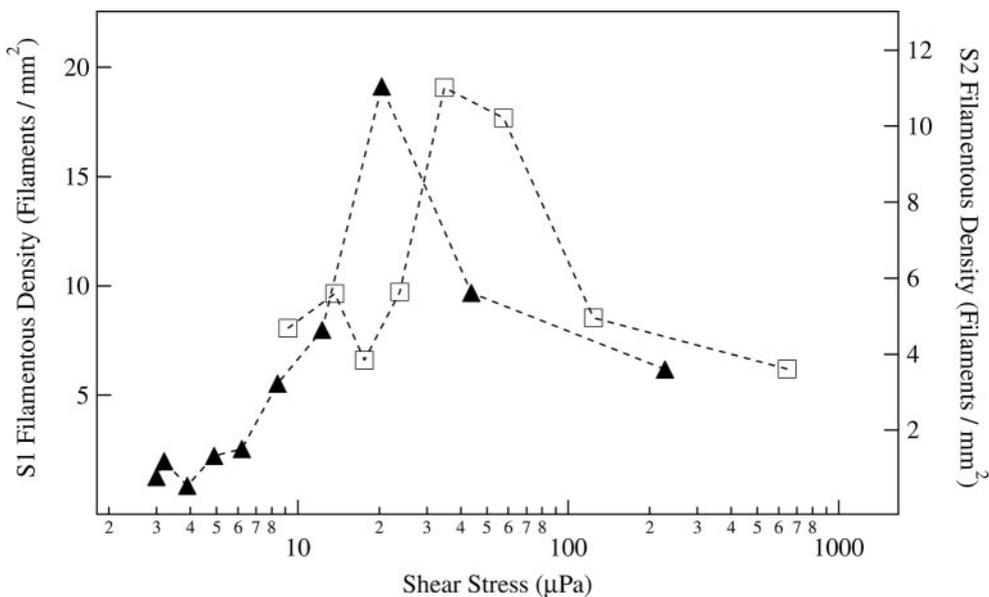

FIG. 4. Filamentous densities for shear stress runs S1 at 0.005 ml/h ($\blacktriangle$) and S2 at 0.010 ml/h ($\square$).
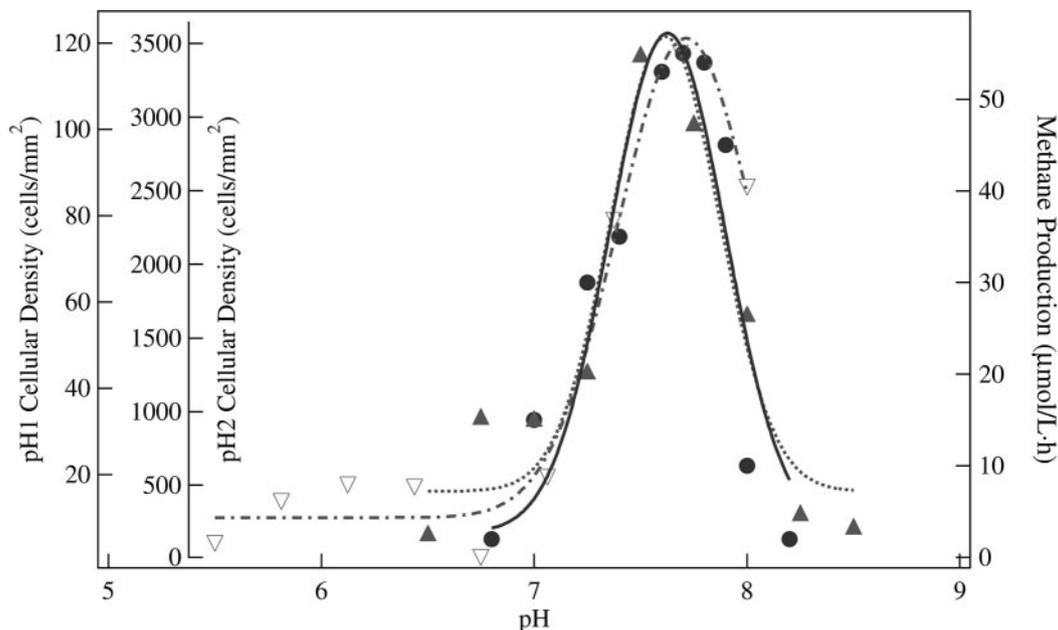
FIG. 5. Data from runs PH1 and PH2 and Huser et al. (16) overlaid with Gaussian curve fits. ●, Huser et al. data; ▽, PH1 with a gradient of pH 5.5 to 8.0; ▲, PH2 with a gradient of pH 6.5 to 8.5.

mum pH was 7.71 for run PH1, 7.62 for run PH2, and 7.63 for Huser et al.'s study [16]).

Ammonia inhibition for *M. concilii*. Based on our total ammonium-N (i.e., the sum of ammonia-N and ammonium-N species) gradient, with nine distinguished total concentrations of between 250 and 2,500 mg NH_4-N/liter, we found optimum

M. concilii growth in the range of 250 to 1,100 mg (total) NH_4-N/liter. The free-ammonia levels were calculated from the total ammonium levels with the ammonia-ammonium chemical equilibrium constant ($pK_a = 8.95$) at a constant temperature of 35°C and a pH of 7.6. The optimum total ammonium-N range corresponds to a free NH_3-N concentration be-
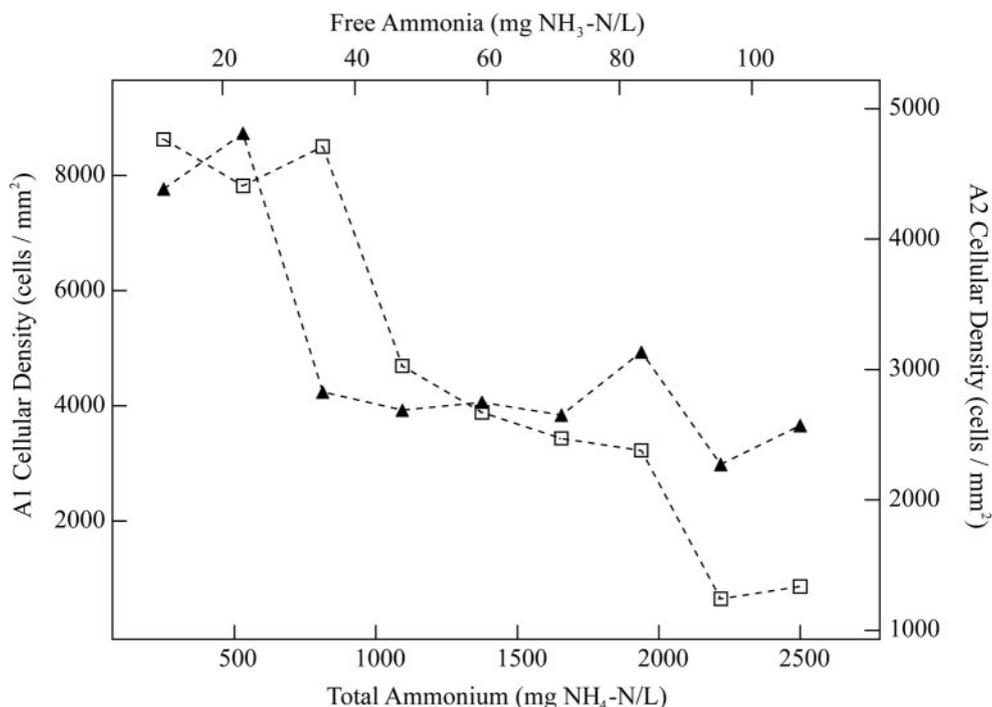

FIG. 6. Cellular density of the gradient channel as a function of ammonia level for runs A1 (▲) and A2 (□) with a gradient of 250 to 2,500 mg NH_4-N/liter.

tween 11 and 47 mg/liter (Fig. 6). Outside of this range, cellular density declined with a sharp drop in growth beyond a total NH_4-N concentration of 1,900 mg/liter (83 mg/liter free NH_3-N). *M. concilii* was found to be the most ammonia-sensitive methanogen among a group of pure cultures, and it was completely inhibited at a concentration of 560 mg (total) NH_4-N/liter at a suboptimal pH level of 7.0 (27). Mesophilic anaerobic digesters with free-ammonia levels of <50 mg/liter typically sustain high levels of the acetoclastic methanogen *M. concilii* (7), and increasing concentrations of ammonia inhibit these methanogens, primarily due to ammonia's effect on intracellular ion exchange (27). Our results are consistent with previous work with unadapted anaerobic digesters, which had shown that total ammonium-N levels above 1,000 to 2,000 mg NH_4-N/liter and 50 to 100 mg free NH_3-N/liter inhibited methanogenesis (7, 10, 14, 17, 30). For successful operation of digesters, it is therefore important to know how *M. concilii* responds to different ammonia levels. At consistently higher ammonia concentrations, anaerobic digesters adapt over some operational period by replacing the abundant *M. concilii* with other methanogens (4, 7, 8).

Our results showcase how the μBR can provide rapid, direct insight into the behavior and growth of anaerobic microorganisms. Due to the low costs of our developed microfluidic device, independent microbiology labs have the ability to study the growth and behavior of other anaerobes in situ. As has been shown already for aerobic microbes, microfluidic technology is useful for studying the effect of changing chemical and physical conditions on the morphology and function of microbes in environmental gradients. In addition, the growth of either anaerobic biofilms or planktonic cells can now be monitored with microfluidics. Our lab plans to use the anaerobic μBR to study syntrophic relationships of archaea and bacteria.

REFERENCES

1. **Absolom, D. R., F. V. Lamberti, Z. Policova, W. Zingg, C. J. van Oss, and A. W. Neumann.** 1983. Surface thermodynamics of bacterial adhesion. Appl. Environ. Microbiol. **46:**90–97.
2. **Angelidaki, I., and B. K. Ahring.** 1993. Thermophilic anaerobic digestion of livestock waste: the effect of ammonia. Appl. Microbiol. Biotechnol. **38:**560–564.
3. **Angenent, L. T., S. Sung, and L. Raskin.** 2004. Formation of granules and *Methanosaeta* fibres in an anaerobic migrating blanket reactor (AMBR). Environ. Microbiol. **6:**315–322.
4. **Angenent, L. T., S. Sung, and L. Raskin.** 2002. Methanogenic population dynamics during startup of a full-scale anaerobic sequencing batch reactor treating swine waste. Water Res. **36:**4648–4654.
5. **Balagaddé, F. K., L. You, C. L. Hansen, F. H. Arnold, and S. R. Quake.** 2005. Long-term monitoring of bacteria undergoing programmed population control in a microchemostat. Science **309:**137–140.
6. **Balch, W. E., and R. S. Wolfe.** 1976. New approach to the cultivation of methanogenic bacteria: 2-mercaptoethanesulfonic acid (HS-CoM)-dependent growth of *Methanobacterium ruminantium* in a pressurized atmosphere. Appl. Environ. Microbiol. **32:**781–791.
7. **Calli, B., B. Mertoglu, B. Inanc, and O. Yenigun.** 2005. Community changes during start-up in methanogenic bioreactors exposed to increasing levels of ammonia. Environ. Technol. **26:**85–91.
8. **Calli, B., B. Mertoglu, B. Inanc, and O. Yenigun.** 2005. Methanogenic diversity in anaerobic bioreactors under extremely high ammonia levels. Enzyme Microb. Technol. **37:**448–455.
9. **Chung, B. G., L. A. Flanagan, S. W. Rhee, P. H. Schwartz, A. P. Lee, E. S. Monuki, and N. L. Jeon.** 2005. Human neural stem cell growth and differentiation in a gradient-generating microfluidic device. Lab Chip **5:**401–406.
10. **De Baere, L. A., M. Devocht, P. Van Assche, and W. Verstraete.** 1984. Influence of high NaCl and NH_4Cl salt levels on methanogenic associations. Water Res. **18:**543–548.
11. **DiLuzio, W. R., L. Turner, M. Mayer, P. Garstecki, D. B. Weibel, H. C. Berg, and G. M. Whitesides.** 2005. *Escherichia coli* swim on the right-hand side. Nature **435:**1271–1274.
12. **Duffy, D. C., J. C. McDonald, O. J. A. Schueller, and G. M. Whitesides.** 1998. Rapid prototyping of microfluidic systems in poly(dimethylsiloxane). Anal. Chem. **70:**4974–4984.
13. **Ferry, J. G.** 1993. Methanogenesis: ecology, physiology, biochemistry & genetics. Chapman & Hall, New York, NY.
14. **Hulshoff Pol, L. W., W. J. de Zeeuw, C. T. M. Velzeboer, and G. Lettinga.** 1983. Granulation in UASB-reactors. Water Sci. Technol. **15:**291–304.
15. **Hungate, R. E.** 1967. A roll tube method for cultivation of strict anaerobes. Methods Microbiol. **3B:**117–132.
16. **Huser, A., K. Wuhrmann, and A. Zehnder.** 1982. *Methanothrix soehngenii* gen. nov. sp. nov., a new acetotrophic non-hydrogen-oxidizing methane bacterium. Arch. Microbiol. **132:**1–9.
17. **Koster, I. W., and G. Lettinga.** 1984. The influence of ammonium-nitrogen on the specific activity of pelletized methanogenic sludge. Agric. Wastes **9:**205–216.
18. **Lau, Y. L., and D. Liu.** 1993. Effect of flow-rate on biofilm accumulation in open channels. Water Res. **27:**355–360.
19. **Leclerc, E., B. David, L. Griscom, B. Lepioufle, T. Fujii, P. Layrolle, and C. Legallaisa.** 2006. Study of osteoblastic cells in a microfluidic environment. Biomaterials **27:**586–595.
20. **Lu, H., L. Y. Koo, W. M. Wang, D. A. Lauffenburger, L. G. Griffith, and K. F. Jensen.** 2004. Microfluidic shear devices for quantitative analysis of cell adhesion. Anal. Chem. **76:**5257–5264.
21. **Munson, B. R., D. F. Young, and T. H. Okiishi.** 2006. Fundamentals of fluid mechanics, 5th ed. John Wiley & Sons, Inc., Hoboken, NJ.
22. **Patel, G. B.** 1984. Characterization and nutritional properties of *Methanothrix concilii* sp. nov., a mesophilic, acetoclastic methanogen. Can. J. Microbiol. **30:**1383–1396.
23. **Qin, D., Y. Xia, and G. M. Whitesides.** 1996. Rapid prototyping of complex structures with feature sizes larger than 20μm. Adv. Mater. **8:**917–919.
24. **Rinzema, A., J. van Lier, and G. Lettinga.** 1988. Sodium inhibition of acetoclastic methanogens in granular sludge from a UASB reactor. Enzyme Microb. Technol. **10:**24–32.
25. **Rittmann, B. E.** 1982. The effect of shear-stress on biofilm loss rate. Biotechnol. Bioeng. **24:**501–506.
26. **Song, J. W., W. Gu, N. Futai, K. A. Warner, J. E. Nor, and S. Takayama.** 2005. Computer-controlled microcirculatory support system for endothelial cell culture and shearing. Anal. Chem. **77:**3993–3999.
27. **Sprott, G. D., and G. B. Patel.** 1986. Ammonia toxicity in pure cultures of methanogenic bacteria. Syst. Appl. Microbiol. **7:**358–363.
28. **van Loosdrecht, M. C. M., J. Lyklema, W. Norde, G. Schraa, and A. J. B. Zehnder.** 1987. The role of bacterial cell wall hydrophobicity in adhesion. Appl. Environ. Microbiol. **53:**1893–1897.
29. **van Schie, P. M., and M. Fletcher.** 1999. Adhesion of biodegradative anaerobic bacteria to solid surfaces. Appl. Environ. Microbiol. **65:**5082–5088.
30. **van Velsen, A. F. M.** 1979. Adaptation of methanogenic sludge to high ammonia-nitrogen concentrations. Water Res. **13:**995–999.